East European Journal of Physics. 1. 393-397 (2024)
DOI:10.26565/2312-4334-2024-1-40 ISSN 2312-4334

SINGLE AND MULTIPHOTON OPTICAL TRANSITIONS IN ATOMICALLY THIN LAYERS OF TRANSITION METAL DICHALCOGENIDES

Rustam Y. Rasulov[a], Voxob R. Rasulov[a]*, Kamolakhon K. Urinova[b], Makhliyo A. Mamatova[a], Bakhodir B. Akhmedov[a]
[a] *Fergana State University, Fergana, Uzbekistan*
[b] *Kokand State pedagogical Institute, Kokand, Uzbekistan*
**Corresponding Author e-mail: vrrasulov83@gmail.com*
Received January 3, 2024; revised February 7, 2024; accepted February 17, 2024

This study explores the optical properties of monolayers from transition metal dichalcogenides (TMDs), materials that have gained attention post-graphene discovery for their unique electronic and optical characteristics. We analyze the crystal structure, Brillouin zones, and electronic band structures of TMD monolayers, laying the foundation to understand their diverse optical phenomena. Special emphasis is placed on the energy spectrum across valleys and the use of an effective Hamiltonian for parallel spin bands. We investigate interband optical transitions, including single-, two-, and three-photon processes, developing equations to calculate transition probabilities that take into account polarization, light frequency, and temperature. Our theoretical analysis, rooted in quantum mechanics, sheds light on the matrix elements that dictate these transitions, underscoring the impact of complex compositions on the optical behavior of TMD monolayers. This work not only advances our understanding of TMD optical properties but also highlights their potential for optoelectronic applications, marking a significant contribution to the field of semiconductor physics.
Keywords: *Polarized photon; Matrix element; Optical transitions; Two-Band approximation; Current carriers; Electron Hamiltonian; Momentum operator; Spin states*
PACS: 71.20. – b, 71.28. + d

INTRODUCTION

The discovery of a method for producing graphene [1] sparked significant interest in the exploration of various two-dimensional (2D) atomic layers of transition metal dichalcogenides (TMDs), which exhibit unique physical properties. Transition metal dichalcogenides are a class of chemical compounds denoted by the formula MX_2, where M represents a transition metal (e.g., Mo, W) and X denotes a chalcogen (e.g., S, Se) [2-5].

In recent years, two-dimensional (2D) structures such as graphene, monolayers of transition metal dichalcogenides (TMDs), monolayers of hexagonal boron nitride, and van der Waals heterostructures based on them have occupied a special place in the field of semiconductor nanosystems [3,4]. The most widely studied representatives among TMDs include MoS_2, $MoSe_2$, WS_2, and WSe_2 monolayers [5-7]. These two-dimensional systems are actively investigated both experimentally and theoretically. It's noteworthy that the boundaries of the hexagonal Brillouin zone are delineated at the $K_\pm$ points. In such scenarios, under the dipole approximation, σ^+ or σ^- polarized light is selectively absorbed in the K_+ or K_- valleys, respectively [6].

Currently, numerous studies focus on the diverse structures of metal dichalcogenides [6]. However, the optical properties of samples with intricate structures remain insufficiently explored. In light of this, the theoretical investigation of single- and multiphoton absorption in monolayers of metal dichalcogenides becomes paramount. This involves a detailed examination of the matrix elements of optical transitions, which constitutes the core subject of this work. Such analysis is crucial for understanding the complex optical behaviors of these materials.

BASIC PROPERTIES OF TMD MONOLAYERS

Fig. 1a,b schematically illustrates the crystal structure and atomic arrangement within TMD monolayers. The monomolecular layer, characterized by the D_{3h} point group, features a horizontal mirror plane that intersects the metal atom layer. The unit cell comprises a metal atom flanked by two chalcogen atoms, positioned in planes above and below the metal plane, respectively. The Brillouin zone is depicted as a regular hexagon (Fig. 1c). The correct exclusion zones at the $K_\pm$ points are identified by the time-reversal symmetry between them. Near these points, the electron dispersion in both the valence and conduction bands exhibits a parabolic shape (Fig. 1d). It is important to note that at the $K_\pm$ points, the band splitting due to spin-orbit coupling vanishes, leading to degeneracy. This symmetry, under the time-reversal operator, allows for the association of states with opposite spins in different valleys.

As a result, we derive the effective Hamiltonian matrix for the K_+ point, which is a 2×2 matrix describing the states with parallel spins in the conduction and valence bands for spin projection s = +1/2 near this point [6], i.e.

Cite as: R.Y. Rasulov, V.R. Rasulov, K.K. Urinova, M.A. Mamatova, B.B. Akhmedov, East Eur. J. Phys. 1, 393 (2024), https://doi.org/10.26565/2312-4334-2024-1-40

$$H_+ = \begin{pmatrix} E_g/2 & \gamma(k_x - ik_y) \\ \gamma(k_x + ik_y) & -E_g/2 \end{pmatrix}. \quad (1)$$

Here, $k_\perp = (k_x, k_y)$ represents the two-dimensional wave vector relative to the γ point in the Brillouin zone, and K_+ signifies a parameter proportional to the interband matrix element of the momentum operator. E_g denotes the band gap. For spin levels within the same valley ($s = -1/2$), the band gap E_g transforms to $E_{g+\Delta}$, where Δ is the sum of the spin-orbit coupling induced energy splittings in the conduction and valence bands. It is important to note that the band gap widths in structures based on molybdenum and tungsten exhibit quantitative differences [5-8]. The effective Hamiltonian for the K_- valley is obtained by the substitution in expression (1) from $k_x \pm ik_y \to k_x \mp ik_y$ [1]. The energy spectrum of an electron, as described by Hamiltonian (1), is given by the following expression, which is also referred to as the Dirac-like energy spectrum [8]:

$$\varepsilon_{\lambda,k} = \lambda\varepsilon_k, \varepsilon_k = \sqrt{(E_g/2)^2 + \gamma^2 k_\perp^2}, \quad (2)$$

where $\tau = +$ corresponds to the conduction band, while $\tau = -$ denotes the valence band. The distinction in band gaps, denoted as $E_\pm(\vec{k}_\perp)$, leads to variations in the energy spectrum, which are depicted in Fig. 1. This figure illustrates how the energy spectrum varies with different band gap values (Fig. 1a) and electron effective masses (Fig. 1b) [5-10]. The diverse band gaps and effective masses across different materials result in significant differences in their electronic properties, as visually represented in these figures.

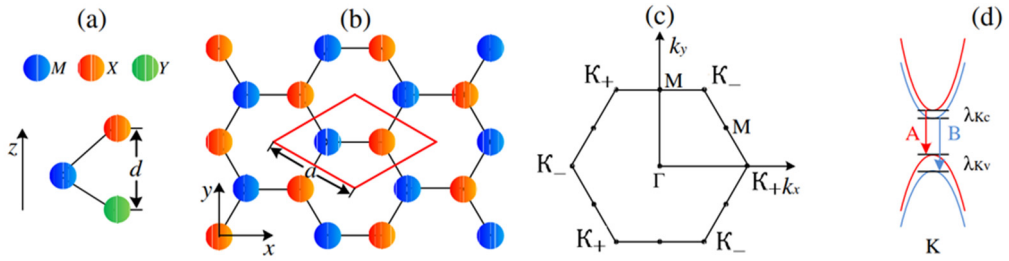

Figure 1. (a) is an MX_2 schematic representation of the monolayer crystal structure of TMD described by the chemical formula. Blue spheres - metal atoms (M), yellow - chalcogen (X), (b) - arrangement of atoms, (c) two-dimensional Brillouin zone, (d) $K_\pm$ image of the energy spectrum near points corresponding to the Brillouin zone and the usual rules for choosing radiation for falls. Here λ_{Kc} and λ_{Kv} are the widths of the spin-orbit bands separating the conduction band and valence band, respectively.

In many instances, to streamline the calculations, the energy spectrum of charge carriers for very small magnitudes of the wave vector (k) can be approximated as follows:

$$\varepsilon_k \approx \frac{E_g}{2} + \frac{\hbar^2 k_\perp^2}{2m^*}, \quad (3)$$

where $m^* = E_g/(2v_0^2)$ is expressed as effective mass, $v_0 = \gamma/\hbar$ quantity per unit speed.

Literature sources, including [4], present varying numerical values for the effective mass of electrons and the band gap in monolayers of metal dichalcogenides. Consequently, Figure 1 illustrates the energy spectra of charge carriers for diverse values of the aforementioned band parameters: it showcases how the energy spectrum's band gap varies with a specific effective mass, alongside the results plotted against the two-dimensional wave vector. Meanwhile, Figure 2 displays the energy spectrum as a function of the effective mass and two-dimensional wave vector, with the band gap held constant.

COMPONENT MATRIX ELEMENTS OF INTERBAND OPTICAL TRANSITIONS

The coefficient of linear-circular dichroism, indicative of the probabilities of optical transitions, is determined by the underlying matrix elements. These elements facilitate a quantum mechanical analysis of such transitions. Moving forward, we will conduct a detailed examination of the matrix elements associated with single- and multiphoton optical transitions, aiming to deepen our understanding of these processes.

Interband single-photon optical transitions. This optical transitions in monolayers of metal dichalcogenides are influenced by the polarization vector $\vec{e}$ of light, its frequency, and the temperature of the sample. Assuming the effect of coherent saturation is negligible, the probability of these optical transitions between the conduction (C) and valence (V) bands can be expressed as:

$$W_{C;V}^{(1)} = \frac{2\pi}{\hbar}\left(\frac{eA_0}{c\hbar}\right)^2 \times \sum_{\vec{k}}\left(f(E_-) - f(E_+)\right)|(\vec{e}\cdot\vec{p})_{cV}|^2\delta(E_+ - E_- - \hbar\omega) \quad (4)$$

is calculated by the expression, here where $(\vec{e}\cdot\vec{p})_{cV}$-pulse operator and the interband matrix element of the scalar product of the polarization vector of polarized light, the remaining quantities are well-known quantities. (1) the eigenfunctions of

the Hamiltonian, i.e., the propagation coefficient of the wave functions of current carriers [10] is determined as noted in the work, and if we pay attention to the fact that the operator $\vec{k}$ impulse is the first-order derivative obtained from relation (1) according to wave vector, then $(\vec{e}\cdot\vec{p})_{cV}$ the matrix element of the operator of single-photon interband optical transitions will be noted in the following form

$$\langle \mathrm{c}|\vec{e}\cdot\vec{p}|V\rangle = \frac{m_0}{\hbar}\left\langle \mathrm{c}\left| e_x\frac{\partial H_+}{\partial k_x} + e_y\frac{\partial H_+}{\partial k_y}\right| V\right\rangle = \frac{m_0}{\hbar}\frac{\gamma}{2\varepsilon(\vec{k})}\left\{e_-\left[\tilde{E}_g + E(\vec{k}_\perp)\right] - \frac{k_-^2}{k_\perp^2}\left[-\tilde{E}_g + E(\vec{k}_\perp)\right]e_+\right\}. \quad (5)$$

Here $p_0 = \frac{m_0\gamma}{\hbar}$, $k_\perp^2 = k_x^2 + k_y^2$, $e_\pm = (e_x \pm ie_y)$. (Diagonal) matrix element of the pulse operator corresponding to single-band networks and single-photon optical transitions:

$$p_{\mathrm{cc}} = -p_{vv} = \vec{e}\cdot\vec{p}_{\mathrm{cc}} = 4\frac{m_0\gamma^2}{\hbar}\frac{\vec{e}_\perp\cdot\vec{k}_\perp}{\sqrt{E_g^2+4\gamma^2k_\perp^2}} = 4p_0\gamma\frac{\vec{e}_\perp\cdot\vec{k}_\perp}{\sqrt{E_g^2+4\gamma^2k_\perp^2}}. \quad (6)$$

is recorded on the form. If we neglect the contribution of the coherent saturation effect, then the squared modulus of the composite matrix element will be written as

$$\left|M_{c;\mathrm{V}}^{(1)}(\vec{k})\right|^2 = \left(\frac{eA_0}{c\hbar}\right)^2 p_0^2\frac{E_g^2+2\gamma^2k_\perp^2}{E_g^2+4\gamma^2k_\perp^2}\left[e_\perp^2 - 2\frac{\gamma^2k^2}{E_g^2+2\gamma^2k_\perp^2}\left(e_x^2-e_y^2\right)\right], \quad (7)$$

Interband two-photon optical transitions. In the general case, two-photon interband optical transitions occur in two stages: at the first stage - interband single-photon optical transitions, then intraband single-photon optical transitions (and vice versa at the second stage) [12]. Then the matrix element of the two-photon optical transition has the form

$$\mathrm{M}_{cV}^{(2)}(\vec{k}_\perp,\vec{e}) = \left(\frac{eA_0}{m_0c}\right)^2\left\{\frac{(\vec{e}\cdot\vec{p})_{cc}(\vec{e}\cdot\vec{p})_{cV}}{E_c(\vec{k}_\perp)-E_V(\vec{k}_\perp)-\hbar\omega} - \frac{(\vec{e}\cdot\vec{p})_{cV}(\vec{e}\cdot\vec{p})_{VV}}{\hbar\omega}\right\}, \quad (8)$$

If we take into account the law of conservation of energy for a given optical transition, then

$$\mathrm{M}_{cV}^{(2)}(\vec{k}_\perp,\vec{e}) = \left(\frac{eA_0}{m_0c}\right)^2\frac{(\vec{e}\cdot\vec{p})_{cc}-(\vec{e}\cdot\vec{p})_{VV}}{\hbar\omega}(\vec{e}\cdot\vec{p})_{cV}. \quad (9)$$

Since the energy spectra of current carriers in the conduction band and valence band differ from each other in sign, the relation $(\vec{e}\cdot\vec{p})_{cc} = -(\vec{e}\cdot\vec{p})_{VV}$ is appropriate. Expression (9) takes into account $E_c(\vec{k}_\perp) - E_V(\vec{k}_\perp) - N\hbar\omega = 0$ relationships associated with N photon absorption of polarized light (from this relationship we obtain $k_\perp(\omega) = \left[(N\hbar\omega)^2 - E_g^2\right]^{1/2}/(2\gamma)$ expressions. Thus, $\mathrm{M}_{cV}^{(2)}(\vec{k}_\perp,\vec{e})$ is determined by the relation

$$\frac{p_{cv}}{\hbar\omega}(p_{cc}-p_{vv}) = \frac{4}{\hbar\omega}\frac{\gamma p_0^2}{\sqrt{E_g^2+4\gamma^2k_\perp^2}}\left(T_+^2e_- - T_-^2e_+\frac{k_-^2}{k_\perp^2}\right)(e_+\cdot k_- + e_-\cdot k_+), \quad (10)$$

where $T_\pm^2 = \left[\left(E_g^2+4\gamma^2k_\perp^2\right)^{\frac{1}{2}} \pm E_g\right] / \left[2\left(E_g^2+4\gamma^2k_\perp^2\right)^{\frac{1}{2}}\right]$, also here the squared modulus of the value $\mathrm{M}_{cV}^{(2)}(\vec{k}_\perp,\vec{e})$ is determined by the expression

$$\left(\frac{4}{\hbar\omega}p_0\gamma\frac{p_0}{\sqrt{E_g^2+4\gamma^2k^2}}\right)^2\left(\Re_{cV}^{(1)} + \Re_{cV}^{(2)} + \Re_{cV}^{(3)}\right), \quad (11)$$

where,

$$\Re_{cV}^{(1)} = 4T_-^4k_\perp^2e_\perp^2\left(2e_xk_x+e_yk_y\right)^2, \Re_{cV}^{(3)} = 4T_+^4e_\perp^2\left(e_xk_x+e_yk_y\right)^2,$$

$$\Re_{cV}^{(2)} = 8\cdot T_+^2\cdot(T_-^2/k_\perp^2)\cdot\left[\left(k_x+k_y\right)e_x - \left(k_xk_y\right)e_y\right]\cdot\left[\left(k_x-k_y\right)e_x + \left(k_x+k_y\right)e_y\right]\cdot\left(e_yk_y+e_xk_x\right)^2.$$

Interband three-photon optical transitions. Now optical transitions involving three photons from the valence band to the conduction band (interband) occur according to the following scheme

$$\left(V,\vec{k}_\perp\right)\to\left(V,\vec{k}_\perp\right)\to\left(V,\vec{k}_\perp\right)\to\left(c,\vec{k}_\perp\right), \left(V,\vec{k}_\perp\right)\to\left(V,\vec{k}_\perp\right)\to\left(c,\vec{k}_\perp\right)\to\left(c,\vec{k}_\perp\right),$$

$$\left(V,\vec{k}_\perp\right)\to\left(c,\vec{k}_\perp\right)\to\left(c,\vec{k}_\perp\right)\to\left(c,\vec{k}_\perp\right), \left(V,\vec{k}_\perp\right)\to\left(c,\vec{k}_\perp\right)\to\left(V,\vec{k}_\perp\right)\to\left(c,\vec{k}_\perp\right).$$

Then the matrix element of interband three-photon optical transitions is represented as

$$M_{cV}^{(3)}(\vec{k}_\perp,\vec{e}) = \frac{(\vec{e}\cdot\vec{p})_{cV}}{4(\hbar\omega)^2}\{2([(\vec{e}\cdot\vec{p})_{cc}^2 + (\vec{e}\cdot\vec{p})_{VV}^2] - 4(\vec{e}\cdot\vec{p})_{cc}(\vec{e}\cdot\vec{p})_{VV} - (\vec{e}\cdot\vec{p})_{cV}(\vec{e}\cdot\vec{p})_{Vc})\}.$$

Then the square of the modulus of the two-photon optical transition $\left(\left|M_{cV}^{(3)}(\vec{k}_\perp,\vec{e})\right|^2\right)$:

$$\left|M_{cV}^{(3)}(\vec{k}_\perp,\vec{e})\right|^2 = \left(\frac{eA_0}{m_0c}\right)^6 \frac{\gamma^6 m_0^6}{16\hbar^6(\hbar\omega)^4 k_\perp^{12}\left(E_g^2+4\gamma^2k_\perp^2\right)^2}(\Re_{41}+\Re_{42}\Re_{43}). \quad (12)$$

here,

$$\Re_{41} = \left(T_-^2k_\perp^4e_\perp^2 - 2\left(\left(e_x^2-e_y^2\right)\left(k_x^2-k_y^2\right)+4k_xk_ye_xe_y\right)k_\perp^2T_+^2\right)\left(E_g^2+4\gamma^2k_\perp^2\right)T_-^2,$$

$$\Re_{42} = \left(T_+^4\left(4\gamma^2k_\perp^2+E_g^2\right)e_\perp^2 - 128\gamma^2\left(e_x^2k_x^2+k_y^2e_y^2\right) - 256\gamma^2k_xk_ye_xe_y\right)k_\perp^4\Big]^2,$$

$$\Re_{43} = \left[T_-^4k_\perp^2e_\perp^2 - 2T_+^2T_-^2k_\perp^2\left(\left(e_x^2-e_y^2\right)\left(k_x^2-k_y^2\right)+4k_xk_ye_xe_y\right) + T_+^4k_\perp^4e_\perp^2\right].$$

CONCLUSIONS

Through this analysis, we have derived matrix element expressions for single-, two-, and three-photon optical transitions between the spin states of the conduction and valence bands. These expressions enable the classification of optical transitions based on the angle between the polarization vectors and wave vectors of the charge carriers, as well as on the band parameters specific to monolayers of transition metal dichalcogenides. Furthermore, they allow for the determination of the spectral and temperature dependences of the coefficients for single- and multi-photon interband absorption of light and linear-circular dichroism. These aspects will be thoroughly investigated in subsequent work.

The theory of nonlinear absorption of polarized radiation in two-dimensional, atomically thin layers of transition metal dichalcogenides has been advanced. It is important to highlight that excluding the effects of coherent saturation from the analysis of interband single-photon absorption of polarized radiation [11] reveals that linear-circular dichroism does not manifest in atomically thin metal dichalcogenides. This observation is attributed to the fact that, under these conditions, the probabilities of single-photon optical transitions are independent of the polarization states of light.

ORCID

Rustam Y. Rasulov, https://orcid.org/0000-0002-5512-0654; **Voxob R. Rasulov,** https://orcid.org/0000-0001-5255-5612
Bakhodir B. Akhmedov, https://orcid.org/0000-0003-4894-3588; **Makhliyo A. Mamatova** https://orcid.org/0000-0001-6980-9877

REFERENCES

[1] K.S. Novoselov, A.K. Geim, S.V. Morozov, D.E. Jiang, Y. Zhang, S.V. Dubonos, I.V. Grigorieva, and A.A. Firsov, "Electric field effect in atomically thin carbon films," science, **306**(5696), 666-669 (2004). https://doi.org/10.1126/science.1102896
[2] N. Huo, Y. Yang, Y.N. Wu, X.G. Zhang, S.T. Pantelides, and G. Konstantatos, "High carrier mobility in monolayer CVD-grown MoS_2 through phonon suppression," Nanoscale, **10**(31), 15071-15077 (2018). https://doi.org/10.1039/C8NR04416C
[3] A. Taffelli, S. Dirè, A. Quaranta, and L. Pancheri, "MoS_2 based photodetectors: a review," Sensors, **21**(8), 2758 (2021). https://doi.org/10.3390/s21082758
[4] G.H. Shin, C. Park, K.J. Lee, H.J. Jin, and S.Y. Choi, "Ultrasensitive phototransistor based on WSe_2–MoS_2 van der Waals heterojunction," Nano Letters, **20**(8), 5741-5748 (2020). https://doi.org/10.1021/acs.nanolett.0c01460
[5] T. Wang, F. Zheng, G. Tang, J. Cao, P. You, J. Zhao, and F. Yan, "2D WSe_2 flakes for synergistic modulation of grain growth and charge transfer in tin-based perovskite solar cells," Advanced Science, **8**(11), 2004315 (2021). https://doi.org/10.1002/advs.202004315
[6] S.H. Su, W.T. Hsu, C.L. Hsu, C.H. Chen, M.H. Chiu, Y.C. Lin, W.-H. Chang, al., "Controllable synthesis of band-gap-tunable and monolayer transition-metal dichalcogenide alloys," Frontiers in Energy Research, **2**, 104870 (2014). https://doi.org/10.3389/fenrg.2014.00027
[7] C. Ernandes, L. Khalil, H. Almabrouk, D. Pierucci, B. Zheng, J. Avila, P. Dudin, et al., "Indirect to direct band gap crossover in two-dimensional $WS_{2(1-x)}Se_{2x}$ alloys," npj 2D Mater. Appl. **5**(1), 7 (2021). https://doi.org/10.1038/s41699-020-00187-9
[8] E.L. Ivchenko, *Optical Spectroscopy of Semiconductor Nanostructures*, (Alpha Science International Ltd., Harrow, UK, 2005).
[9] R.Y. Rasulov, V.R Rasulov, N.Z. Mamadalieva, and R.R. Sultanov, "Subbarrier and Overbarrier Electron Transfer through Multilayer Semiconductor Structures," Russian Physics Journal, **63**, 537-546 (2020). https://doi.org/10.1007/s11182-020-02067-7
[10] M.M. Glazov, *Electron and Nuclear Spin Dynamics in Semiconductor Nanostructures*, (Oxford University Press, Oxford, 2018). https://doi.org/10.13140/RG.2.2.18718.56640
[11] V.R. Rasulov, R.Ya. Rasulov, and I. Eshboltaev, "Linearly and circular dichroism in a semiconductor with a complex valence band with allowance for four-photon absorption of light," Physics of the Solid State, **59**(3), 463–468 (2017). https://doi.org/10.1134/S1063783417030283
[12] R. Rasulov, V. Rasulov, and I. Eshboltaev, "On the Theory of the Ballistic Linear Photovoltaic Effect in Semiconductors of Tetrahedral Symmetry Under Two-Photon Absorption," Russian Physics Journal, **59**, 92–98 (2016). https://doi.org/10.1007/s11182-016-0742-7

ОДНО-ТА БАГАТОФОТОННІ ОПТИЧНІ ПЕРЕХОДИ В АТОМНО ТОНКІХ ШАРАХ ДИХАЛЬКОГЕНІДІВ ПЕРЕХІДНИХ МЕТАЛІВ

Рустам Я. Расулов[a], Вокхоб Р. Расулов[a], Камолахон К. Урінова[b], Махліє А. Маматова[a], Баходір Б. Ахмедов[a]

[a] *Ферганський державний університет, Фергана, Узбекистан*

[b] *Кокандський державний педагогічний інститут, Коканд, Узбекистан*

У статті обговорюється виробництво та властивості двовимірних атомних шарів дихалькогенідів перехідних металів (ТМД) з акцентом на оптичних властивостях моношарів. Він починається зі вступу до відкриття методів виробництва графену та подальшого інтересу до TMD. Деталізовано основні властивості моношарів ТМД, їх кристалічну структуру та зону Бріллюена. У статті досліджено енергетичний спектр електронів у різних долинах та ефективний гамільтоніан, що описує стани в паралельних спінових зонах. Обговорення поширюється на матричні елементи міжзонних оптичних переходів, включаючи одно-, дво- та трифотонні переходи. Наведено рівняння для розрахунку ймовірностей оптичних переходів, включаючи такі фактори, як вектор поляризації, частота світла та температура зразка. Викладено теоретичний аналіз складових матричних елементів для цих переходів, наголошуючи на квантово-механічних аспектах. Стаття сприяє дослідженню оптичної поведінки моношарів дихалькогенідів перехідних металів (ТМД), зокрема в структурах складного складу.

Ключові слова: *поляризований фотон; матричний елемент; оптичні переходи; двозонне наближення; носії струму; електронний Гамільтоніан; оператор імпульсу; спінові стани*